VNUHCM Journal of Engineering and Technology 2026, (2): 2800-2810

Open Access Full Text Article

Research Article

Molecular docking, DFT study of some modified curcumins as potential anticancer agents on CXCR2 receptor

Le Vu Phuc , Tran Thi Thu Hanh *

Use your smartphone to scan this QR code and download this article

ABSTRACT

Natural compounds with potential applications in treating complex diseases such as cancer are increasingly garnering attention in medical research. The utilization of computational modeling methods is becoming more prevalent in studying these compounds, facilitating the selection of promising molecular frameworks for therapeutic purposes. Curcumin, a molecule with numerous modified and analogous structures, is used to anticipate potential pharmaceutical compounds using computational calculation methods. This study aims to employ several structures, including curcumin, demethoxycurcumin (DMC), bisdemethoxycurcumin (BDMC), dihydrocurcumin (DHC), and notably tetrahydrocurcumin (THC), to forecast the potential inhibition of the CXCR2 receptor through the DFT and molecular docking methodologies. Molecular docking and DFT calculations play crucial roles in predicting activity stability and electron properties, aiding in better understanding the compounds' structures. In this article, the Density Functional Theory (DFT) method will be employed to optimize the structure and calculate various quantum parameters. Subsequently, the optimized structure will undergo 1H NMR spectroscopy computation and comparison with experimental data to evaluate the proximity to experimental reality. The Ligands will then be subjected to docking with the CXCR2 protein to assess their impact on this protein. The research delineates the noteworthy inhibitory efficacy of THC on CXCR2, facilitated by the formation of pi-sigma bonds within the receptor's binding pocket. These findings are expected to guide forthcoming investigations aimed at advancing THC as a prospective pharmaceutical candidate in the future. This article comprises the following sections: an introduction section providing an overview of the natural molecules which are called the ligands, and target protein; the computational methods section outlining the computational techniques to be utilized in the study that include DFT and molecular docking with Autodock Vina software; and a results section presenting the findings obtained during the research process.

Key words: Drug design, molecular docking, natural compounds, curcumin derivatives, CXCR2 inhibition

Faculty of Applied Science, Ho Chi Minh City University of Technology (HCMUT), VNU-HCM, Ho Chi Minh City, Vietnam

Correspondence

Tran Thi Thu Hanh , Faculty of Applied Science, Ho Chi Minh City University of Technology (HCMUT), VNU-HCM, Ho Chi Minh City, Vietnam

Email: thuhanhsp@hcmut.edu.vn

History

- Received: 26-8-2024
- Revised: 23-09-2025
- Accepted: 21-10-2025
- Published Online: 07-05-2026

DOI : https://doi.org/10.32508/vnuhcmj-et.v9i1.1437

Check for updates

VNUHCM PRESS

INTRODUCTION

Natural compounds such as paclitaxel, cannabinoids, and curcumin showed the activities against currently difficult-to-treat diseases such as Alzheimer's and cancer. [1] There were many in vitro and in vivo studies on these compounds. Curcumin has shown promise as a potential therapeutic compound and was widely used in traditional medicine for several diseases. [2,3]

Curcumin is the main active ingredient extracted from turmeric (Curcuma longa). However, other curcuminoids, such as demethoxycurcumin (DMC) bisdemethoxycurcumin (BDMC), and dihydrocurcumin (DHC), are also present in turmeric extract. [4,5] There was a study of isolating active compounds from Chinese turmeric (Curcuma wenyujin) discovered tetrahydrocurcumin (THC), a white powder derivative of curcumin (compared with yellow pigment in turmeric). THC boasts impressive anti-inflammatory, antioxidant, and anticancer properties. Compared to curcumin, THC offered better stability, bioavailability, and antioxidant activity, potentially making it a more effective weapon against cancer. THC actsed through various mechanisms, including reducing oxidative stress, aiding detoxification, and directly combating cancer cells. While research on THC's potential is promising, further studies are needed to confirm its safety and efficacy in humans. [6]

Notably, THC is both a natural product and a key metabolite of curcumin in our bodies. It surpasses curcumin in chemical stability, bioavailability, and antioxidant activity. This translates to a multi-pronged attack against cancer, with THC influencing oxidative stress, detoxification, inflammation, cell growth, spread, death, and even the immune system. While THC's potential is undeniable, further research is crucial to definitively assess its effectiveness and safety for human use. [4,7,8]

Cite this article : L V P, T T T H. **Molecular docking, DFT study of some modified curcumins as potential anticancer agents on CXCR2 receptor**. *VNUHCM J. Eng. Technol.* 2026; (2):2800-2810.

G-protein coupled receptors (GPCRs) act as the body's cellular control panel, with a massive family of these transmembrane proteins regulating everything from hormone response to cell migration.[9]

They are a goldmine for drug discovery, as most medications today work by influencing them. Within the GPCR family, CXCR1 and CXCR2 have emerged as particularly intriguing targets. These receptors play a critical role in the fate of cancer cells, influencing their growth, programmed cell death (apoptosis), and the formation of new blood vessels (angiogenesis) that feed tumors.[10]

While the 3D structure of CXCR2 was known, allowing for more targeted computer-aided drug design, the structure of CXCR1 remains a puzzle. This puts CXCR2 at the forefront of current research efforts, with scientists using computational modeling to design drugs that specifically target this receptor and potentially disrupt vital processes in cancer cells. However, research on CXCR1 continues, and unraveling its structure could unlock a new wave of targeted therapies for cancer.[11]

This article uses quantum chemical tools to optimize the structures of curcumin and its derivatives. Several quantum chemical parameters were calculated using the simulation method. These structures were then docked with the CXCR2 receptor to assess their potential for anticancer activity against this receptor.

METHODS

Cytotoxic activity assay

The cytotoxic activity assay was performed in the research of Sandur[4]

Structures Optimization

Orca software version 4.0 was employed alongside DFT calculations to optimize the structures. The 6-311G* basis set and the B3LYP exchange-correlation functional were utilized.[12,13] Similar to Gaussian, Orca was used to compute various chemical parameters including the energy of the highest occupied molecular orbital (E_{HOMO}), the energy of the lowest unoccupied molecular orbital (E_{LUMO}), the bandgap ($E_{gap} = E_{HOMO} - E_{LUMO}$), global hardness ($\eta$), global softness (S), and dipole moment (μ).

Calculating energy using exchange function BL3P and basic sets 6-311G*, as outlined in this article, may not yield results that are superior to those obtained with other higher-level methods, such as WTF or PBE0. Nonetheless, for the comparison of organic molecules in this study, it is practical to employ a cost-effective computational approach like DFT. Furthermore, optimized methods such as RI-MP2, HF-3c and DFT-3c can be utilized, offering both low computational costs and satisfactory optimization outcomes.[14]

The Orca software has the capability to optimize molecular structures using quasi-Newton updates with the well-known Broyden-Fletcher-Goldfarb-Shanno (BFGS) algorithm, and Powell or Bofill updates.

In this article, we employ the default methods of Orca, quasi-Newton method with BFGS updates. The version is Orca 4.0.[15]

The following section will provide an overview of the theoretical foundations of this computational method.

Quasi newton procedure and BFGS optimization

Quasi Newton Procedure

Optimization problems in computational molecular simulation generally involve convex functions, Newton's methods showed more advantages compared to gradient descent approaches. However, the Newton optimization method had limited in costly in computation, and it is uncommon fozr contemporary computational systems to accommodate these demands. This challenge can be mitigated by a novel approach that integrates gradient descent with Newton's optimization methods, this is called quasi-newton methods. In the subsequent section, we will review key principles of quasi-Newton optimization methods.

As we know, in Newton's method, the computational expense arises primarily from calculating the Hessian and its inverse at each iteration, especially as the dimensionality increases significantly. In quasi-Newton methods, instead of computing the actual Hessian values, we use an approximate representation with a positive matrix B (which must be positive definite since we are working with convex functions). This approach reduces the computational cost at each iteration, as we only need to approximate rather than calculating the entire Hessian at each stage.

We have the optimization equation in Newton's method:

$$X_{k+1} = X_k - [H(X_k)]^{-1} \nabla f(X_k) \quad (1)$$

XK, Xk+1: Variables in k and k+1 point, X have n-dimensional

F(Xi): Target function

H(Xk): Hessian of Variable Xk

In quasi-Newton method, we had:

$$B_{k+1}[X_{k+1} - X_k] = \nabla f(X_{k+1}) - \nabla f(X_k) \quad (2)$$

We could consider $\nabla f(X_{k+1}) - \nabla f(X_k)$as a finite integral of the gradient function, equation (2) can be

rewritten as follows $y_k = \nabla f(X_{k+1}) - \nabla f(X_k)$and $\triangle X_k = X_{k+1} - X_k$

$$B_{k+1}\nabla X_k = y_k \tag{3}$$

Since, as previously assumed, matrix B will take positive values, leading to $y_k \Delta X_k > 0$.

Returning to the secant equation in the one-dimensional case, we have:

$$f''(x_{k+1})(x_{k+1} - x_k) = f'(x_{k+1}) - f'(x_k), \tag{4}$$

And the curvature condition satisfies the following condition:

$\frac{f'(x_{k+1}) - f'(x_k)}{x_{k+1} - x_k} > 0$

From there, we substitute f" into the Newton's method equation:

$$x_{k+1} = x_k - f'(x_k)\frac{x_k - x_{k+1}}{f'(x_k) - f'(x_{k+1})} \tag{5}$$

At this point, we have a method to achieve faster optimization by using approximate second-order derivatives from previous steps to accelerate convergence. At each iteration k+1, we create an approximate second derivative by taking the first derivatives from two iterations, k and $k-1$.

This is a subclass of the quasi-Newton method, which approximates the second-order derivatives using first-order derivatives from previous steps. This is also known as the secant method.

In the n-dimensional problem, let B be a symmetric $n \times n$ matrix with n(n+1)/2 components. If we adopt a similar approach as in the one-dimensional space, we will invert B from equation (3) and substitute it into equation (2). However, we can only determine n components from this equation, leaving n(n−1)/2 components undetermined.

The secant equation in the quasi-Newton method needs to be generalized in n-dimensional space, rather than simply using finite differences as in equations (4) and (5). As a result, the quasi-Newton method will introduce additional constraints. Nonetheless, in general, the approximate values of B will still be informed by the gradient values computed in previous steps.

Many quasi-Newton methods have been developed, and in the Orca software, the quasi-Newton method used is based on the BFGS algorithm.

Structural optimization using the BFGS algorithm

As mentioned above, quasi-Newton methods with n>1 dimensions require additional constraints to determine the undetermined components. One constraint is that matrix B must be positive definite and symmetric. Another possible constraint to consider is that matrix B_k must be as close as possible to matrix B_{k+1} in each iteration.

$$\begin{aligned} &min_{B_{k+1}} = \left\| {B^{-1}}_{k+1} - B_k^{-1} \right\| \\ &{B^T}_{k+1} = B_{k+1} \\ &B_{k+1}\nabla X_k = Y_k \end{aligned} \tag{6}$$

In the BFGS algorithm, we will use the Frobenius norm for the norm value:

$$\|A\|_F = \sqrt{\sum_i^m \sum_j^n \left|a_{ij}\right|^2} \tag{7}$$

This norm is simply calculated as the sum of the absolute values of the matrix components. The solution to equation (6) will not be addressed here; instead, we will focus on estimating the values of Bk+1in each iteration using the following equation:

$$B_{k+1} = B_k + U_k + V_k \tag{8}$$

"In which Uk and Vk are two rank-one matrices used to approximate Bk+1

The two matrices U and V can be expressed as U=auuT and V=$bvvT$, where u and v are two linearly independent non-zero vectors."

$$B_{k+1} = B_k + auu^T + bvv^T \tag{9}$$

Applying the quasi-Newton equation, we have:

$$B_{k+1}\triangle X_k = B_k \triangle X_k + auu^T \triangle X_k + bvv^T \triangle X_k = Y_k \tag{10}$$

We choice u=yk, v= BkΔXk

$$\begin{aligned} &B_k \triangle X_k + a y_k y_k^T \triangle X_k + b B_k \triangle X_k \triangle {X^T}_k \triangle B_k^T \triangle X_k = y_k \\ &y_k(1 - a{y^T}_k \triangle X_k) = B_k \triangle X_k (1 + b \triangle X_k \triangle X_k^T B_k^T) \\ &\Rightarrow a = \frac{1}{y_k^T \triangle X_k},\ b = -\frac{1}{\triangle X_k \triangle X_k^T B_k^T} \end{aligned} \tag{11}$$

Substituting a and b into equation (9), we obtain the BFGS update

$$B_{k+1} = B_k + \frac{y_k y_k^T}{y_k^T \triangle x_k} - \frac{B_k \triangle X_k \triangle X_k^T B_k}{\triangle X_k^T B_k \triangle X_k} \tag{12}$$

From this idea, we can utilize the previous results to compute in each subsequent iteration to save computational costs, instead of using the Newton method.

Molecular docking

In this study, computational methods were employed to investigate the interactions between certain compounds and the CXCR2 protein, a potential target for inhibition. The process involved several software programs and techniques. Firstly, the Molecular Graphic Laboratory (MGL) and the Orca quantum software programs were utilized for computational analyses. These programs are commonly used

for molecular modeling and quantum chemical calculations, respectively. To optimize the geometries of the compounds, the Density Functional Theory (DFT) method was employed, using the (6-311G) basis set with the Orca quantum package. DFT is a quantum mechanical modeling method used to study the electronic structure of molecules, while the basis set specifies the mathematical functions used to represent the electron density. The CXCR2 protein structure, essential for understanding its interaction with the compounds, was obtained from the Research Collaborator for Structural Bioinformatics (RCSB) database using the entry code (6lfl). This database provides access to experimentally determined structures of biological macromolecules. To determine the binding locations of the compounds with the CXCR2 protein, Autodock tools (ADT, version 1.5.6) were utilized. Autodock is a widely used software for molecular docking simulations, which predicts the preferred orientation and conformation of a ligand (the compound) when bound to a receptor (the protein). During the computation process, both polar hydrogen atoms and Gasteiger charges were taken into consideration. Gasteiger charges are partial atomic charges used to represent the distribution of electrons in a molecule. In cases where the root of the molecule was not specified by the user, Autodock automatically selected it using an automated procedure. This root selection is crucial for defining the orientation of the ligand within the binding site of the protein. After determining the binding locations, Autogrid (version 4.2.6) was used to calculate atomic affinity maps and electrostatics for each ligand atomic group. This step provides insights into the energetics of ligand-protein interactions, aiding in the interpretation of docking results. Finally, the Discovery Studio Visualizer program was used to visualize the interactions between the protein and its complexes. Discovery Studio Visualize is a molecular visualization software that allows for the visualization and analysis of protein structures and their interactions with ligands.

HOMO, LUMO, and Chemical Reactivity

Understanding a molecule's behavior often involves examining its highest occupied molecular orbital (HOMO) and lowest unoccupied molecular orbital (LUMO).

HOMO: This orbital holds the electrons that can most readily participate in bonding with other molecules. Its energy represents the molecule's ionization potential, which is the minimum energy required to remove an electron.

LUMO: This orbital represents the easiest location for the molecule to accept an additional electron. Its energy reflects the molecule's electron affinity or the energy changes when it gains an electron.

The E_{HOMO} - E_{LUMO} gap, the energy difference between these two orbitals, is a crucial indicator of a molecule's reactivity. A large E_{HOMO}- E_{LUMO} gap signifies greater stability. This is because a significant energy jump is needed to excite an electron from bonding (HOMO) to a non-bonding state (LUMO), making the molecule less reactive.

Furthermore, the E_{HOMO}- E_{LUMO} gap is linked to a molecule's polarizability. Molecules with a smaller gap are more susceptible to external electric fields, allowing for easier distortion of their electron distribution. This concept aligns with the idea that hardness (resistance to change) is related to polarizability (ease of distortion) as proposed by Parr and Pearson (1984) [16]

In Orca version 4.0, by employing methods such as Density Functional Theory (DFT) or Hartree-Fock (HF), ORCA solves the Schrödinger equation to compute the electronic wavefunctions of the molecule. It then constructs either a Fock or Kohn-Sham matrix, incorporating factors such as kinetic energy, electron-nucleus interactions, and electron-electron interactions. The matrix is diagonalized to obtain the molecular orbital energies, where the HOMO is identified as the highest energy orbital occupied by electrons, and the LUMO as the lowest unoccupied orbital. These energy values are presented in the output file, specifically in the "ORBITAL ENERGIES" section. [15]

Dipole Moments and Molecular Polarity

The dipole moment (μ) is a measure of a molecule's overall polarity. It arises due to the uneven distribution of electrical charge within the molecule. Imagine a molecule as a collection of positive and negative charges associated with its atoms. If these charges are perfectly balanced and symmetrical, the molecule will have no net dipole moment and be considered nonpolar. However, in most cases, the distribution is unequal, creating a separation of positive and negative regions. This separation creates a polar molecule, with a positive end and a negative end.

The magnitude of the dipole moment depends on two factors:

Charge Difference: The greater the difference in electronegativity between bonded atoms, the larger the separation of charge and the stronger the dipole moment.

Bond Distance: The distance between the positive and negative regions also plays a role. A larger distance

between the partial charges leads to a greater dipole moment.

Individual bonds within a molecule can also have dipole moments, reflecting the polarity of that specific bond. The overall molecular dipole moment is determined by considering the vector sum of these individual bond dipole moments. If the bond dipoles cancel each other out due to their

arrangement, the molecule will have no net dipole moment.

ORCA software calculates the dipole moment by analyzing the distribution of electric charge within a molecule. This calculation is based on the wavefunction generated by the selected quantum chemical method, such as DFT or Hartree-Fock, as well as the positions and charges of the nuclei. The dipole moment μ is determined using the following formula:

$$\overrightarrow{\mu} = \sum_i Z_i \overrightarrow{R_i} - \int \rho(\overrightarrow{r}) \overrightarrow{r} d\overrightarrow{r} \quad (13)$$

Where Z_i is the charge of nucleus i

R_i is its position vector, and $\rho(r)$ is the electron density at position r.

ORCA calculates the dipole moment by assessing the difference between the positive nuclear charge center and the negative electronic charge distribution. The resulting dipole moment vector, along with its magnitude, is reported in the output file under the section titled "DIPOLE MOMENT". This section provides the individual components of the dipole moment along the x, y, and z axes, as well as the total magnitude, which is typically expressed in Debye units. [15]

Ionization Potential and Reactivity

Ionization potential (IP) refers to the minimum amount of energy required to remove an electron from an atom or molecule. This process can be represented by the equation:

$$X + E \rightarrow X^+ + e^- \quad (14)$$

where X represents the atom or molecule, E is energy, X^+ is the resulting positively charged ion (cation), and e^- is the ejected electron.

The energy of the HOMO (highest occupied molecular orbital) is often used as an approximation of IP. This is because the HOMO houses the electrons that are easiest to remove.

The IP of an atom or molecule is closely linked to its chemical reactivity. Here's the connection:

High IP: Removing an electron requires a significant amount of energy, indicating a stable electronic configuration. Molecules with high IP tend to be less reactive because they hold onto their electrons tightly.

Low IP: Extracting an electron is easier due to the lower energy requirement. Molecules with low IP are generally more reactive as they can readily lose electrons and participate in chemical reactions.

Electron affinity

Electron affinity (EA) reflects how much energy a system releases when it gains an electron. Think of it as the attractiveness of a system for an extra electron. The lower the EA (more negative), the stronger the attraction and the more energy is released upon gaining the electron.

This concept is related to the lowest unoccupied molecular orbital (LUMO) of the system. The LUMO represents the energy level an incoming electron would occupy. A lower LUMO energy suggests a more stable position for the added electron, leading to a larger energy release (more negative EA)

Chemical hardness

Chemical hardness (η) reflects how difficult it is to remove or add an electron to an atom. A higher hardness indicates greater resistance to change. It is calculated using the ionization energy (IE) and electron affinity (EA) of the atom through the following equation:

$$\eta = (IE - IA)/2 \quad (15)$$

In simpler terms, imagine chemical hardness as a measure of how tightly an atom holds onto its electrons. Harder atoms have a larger energy gap between losing an electron (ionization energy) and gaining one (electron affinity). This makes them less reactive because it takes more energy to either remove or add an electron. The equation combines both ionization energy and electron affinity to provide a single value representing this hardness.

Chemical softness

Chemical softness (S) is the opposite of chemical hardness (η). It describes how easily an atom or molecule can accept electrons. Soft atoms or molecules are more like electron sponges, readily accepting them and releasing energy in the process. They tend to be more reactive because gaining an electron doesn't require much energy.

Chemical softness is calculated as the inverse of hardness:

$$S = 1/\eta \quad (16)$$

Electronegativity (χ)

Electronegativity (χ) is a concept used in chemistry to describe an atom's ability to attract electrons towards itself when forming a chemical bond. Imagine it as a measure of how "electron hungry" an atom is.

Atoms with high electronegativity tend to pull electrons closer to themselves in a bond, creating an uneven distribution of electrical charge.

Interestingly, electronegativity can be calculated using a combination of an atom's ionization energy (IE) and electron affinity (EA) through the following equation:

$$X = (IE + EA)/2 \quad (17)$$

RESULTS

Cytotoxic activity

In the study of Santosh K.Sandur et al. the anti-inflammatory and anti-proliferative activities of various analogs of curcumin found in turmeric, including demethoxycurcumin (DMC), bisdemethoxycurcumin (BDMC), tetrahydrocurcumin (THC), and turmerones, compared to curcumin itself. The findings revealed that curcumin exhibited the highest potency in suppressing tumor necrosis factor (TNF)-induced nuclear factor-kB (NF-kB) activation, followed by DMC and then BDMC. This suggested that the presence of methoxy groups on the phenyl ring plays a critical role in this activity. THC, which lacks conjugated bonds in the central seven-carbon chain, showed complete inactivity in suppressing NF-kB activation, while turmerones also failed to inhibit this process. The suppression of NF-kB activity was associated with the down-regulation of various NF-kB-regulated genes, including cyclooxygenase-2, cyclin D1, and vascular endothelial growth factor. However, the methoxy groups seemed to have a minimal role in the growth-modulatory effects of curcumin, as the suppression of cell proliferation by curcumin, DMC, and BDMC was comparable. THC and turmerones were also active in suppressing cell growth but to a lesser extent than curcumin, DMC, and BDMC. Interestingly, there was no observed relationship between any of the curcuminoids and reactive oxygen species (ROS) production, indicating that the anti-inflammatory and anti-proliferative activities of these compounds are not dependent on their ability to modulate ROS status. In summary, the study demonstrated that different analogs of curcumin present in turmeric exhibit variable anti-inflammatory and anti-proliferative activities, with methoxy groups playing a crucial role in NF-kB suppression but not necessarily in cell proliferation inhibition. [17]

Integrate theoretical and experimental findings

This segment integrates experimental data to refine theoretical values, as outlined in the reference. [18] Compound 2 served as the benchmark in this study. Employing the DFT method and (PCSSEG-2) basis set in the solvent DMSO, nuclear magnetic resonance (NMR) values were predicted. The comparison between predicted and experimental results is presented in Table 1. Fig. 2 illustrates the coefficient of determination (R^2), indicating the degree of convergence between the two sets of values. A higher R2 value, approaching 1, signifies better convergence. In this experiment, the R^2 value was determined to be 0.9992 (Fig. 2), indicating a high level of convergence. Thus, the theoretical component of this study affirms the accuracy of the estimations.

^{1}H NMR theoretically and experimentally values of compound 2

Table 1: ^{1}H NMR theoretically and experimentally values ofcompound 2

Functional groups	Theoretical values (ppm)	Experimental values (ppm)
m,6H,OCH3	3,93	3,84
m,4H,ArH	7,51	7,09
bs,5H,CH2	7,21	6,79

Activity and the 3D structures of compounds

The structures of curcumin and its derivatives with their corresponding names in Figure 1 were obtained from the PubChem chemical formula database. [19,20] These 2D structures were subsequently optimized to obtain the structures shown in Figure 3. The optimized values will be analyzed in the following sections.

The activity of certain chemicals is discussed concerning their physical properties, as outlined in Table 2. The E_{gap} value will be in the order of 5 > 3 > 1 > 4 > 2 showing a specific pattern of activity. Ionization energy (IE) was noted to influence the compounds' effectiveness, with lower IE correlating with higher activity. Ionization energy (IE) values were arranged in the following order 3>4>1>5>2. Hardness and global softness were also considered, with specific sequences indicating reactivity and stability. The hardness values were in the following order: 3>4>1>2>5.

The chemical softness (S), as identified by Radhi et al. (2020), acts as the counterpart to global toughness. A molecule's degree of softness significantly impacts both its stability and reactivity and this is the most important factor, with the sequence based on S being: 5>2>1>4>3.

The dipole moment (μ) will affect the inhibitory ability of the receptor, and has the following order: 5>2>4>3>1, we can see that active ingredient 5 (THC)

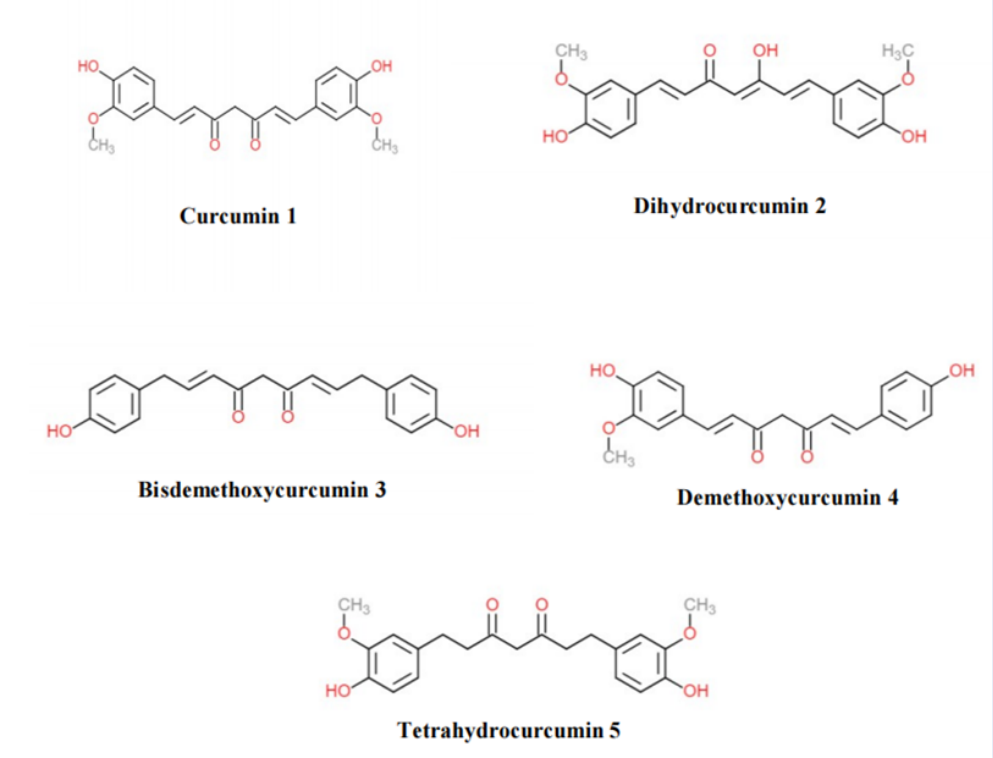

Figure 1: 2Dstructures for the study of compounds (1–5). [Source: Authors]

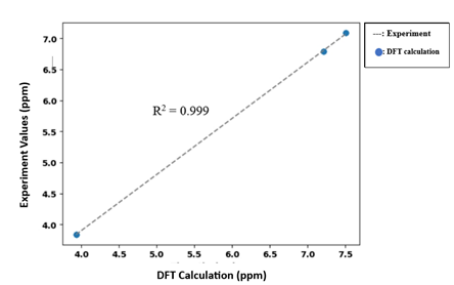

Figure 2: .NMR values in theoretical and experimental study for the compound 2. [Source:Authors]

has strong activity, then compound 2 (DHC), then compound 4 (DMC).

The geometric structure of the compounds was optimized using the BLY3P/6-31G(d,p) method in the Orca program package. The structures obtained all have positive vibration frequencies, proving that this is a structure with minimum energy on the potential energy surface (Figure 3).

The structure of the receptor protein coded 6lfl has a 3D structure including the active region shown in Figure 4.

Molecular docking

The receptors exhibit active sites capable of both accepting and donating hydrogen bonds. The compounds under investigation feature carbon atoms with electron donor density, crucial for hydrogen bond formation (Fig. 5). This electron density is typically accommodated by other atoms.

Moreover, the substances studied exhibit dual hydrophilic and hydrophobic traits. As illustrated in Fig. 6, the hydrophilic aspect, denoted by the color blue, contrasts with the hydrophobic characteristics depicted by the color brown, each having unique values.

In the 2D analysis focusing on the binding region, compounds 1, 2, and 5 were evaluated. Structure 5 exhibits the highest count of bonds and bond types compared to the other two structures.

Specifically, compound 5 forms bonds with SER, VAL, GLU, and TYR, encompassing van der Waals, hydrogen bonds, Pi-Donor, and Pi-sigma bonds, although pi bonds are weaker than sigma bonds themselves, pi bonds constitute part of multiple bonds along with sigma bonds. The combination of pi and sigma bonds is stronger than any individual bond within those

two types. In contrast, structure 1 features bonds including van der Waals, hydrogen, carbon-hydrogen, and pi donor hydrogen bonds with amino acids like THR, SER, and ASP. Structure 2, however, presents only three bond types: hydrogen, van der Waals, and carbon-hydrogen bonds, engaging with amino acids ASP, Gly, and Val at two connection points. This analysis underscores that structure 5 exhibits a superior potential for binding to the receptor under investigation compared to the other structures analyses. Results from ^{1}H NMR validation supported the docking values obtained for R^2. Additionally, Density Functional Theory (DFT) studies were conducted to explore the physical properties of these compounds, confirming the significant activity of compounds 5, 2, and 4. The docking study highlights the potential of these compounds as anticancer agents, with compounds 1, 2, and 5 showing superior efficacy compared to compounds 3, 4. These findings drive ongoing research focused on developing potent anticancer agents through the modification of natural products. Molecular docking and DFT calculations play crucial roles in predicting activity stability and electron properties, aiding in better understanding the compounds' structures. Further investigations are underway to elucidate the mechanisms of action and develop derivatives aimed at enhancing anticancer inhibitory activity.

When we optimized the structure of five molecules using the DFT (Density Functional Theory) computational method, we observed that, although these structures initially shared a similar form—comprising two six-membered aromatic rings connected by a carbon chain—there were slight differences in functional groups and atoms, leading to variations in the final structure after relaxation. Specifically, the angle between the two six-membered rings varied. Upon docking these structures with the target protein, we found that for the three molecules with the best binding affinity, the angle between the two rings was either 180°—as seen in the curcumin molecule—or formed an acute angle, as observed in the THC and DHC molecules, which allowed for optimal interaction with the protein's binding site.

Among the two configurations of THC and DHC, we noted that the position of the functional groups significantly influenced ligand binding to the target. In this study, the different distribution of oxygen atoms in THC compared to DHC, specifically along the carbon chain connecting the two six-membered rings, resulted in the formation of a pi-sigma interaction, which was absent in the other two molecules. This demonstrates that even small variations in molecular design can lead to substantial differences in ligand-receptor interactions.

CONCLUSIONS

The potential anticancer role of novel compounds 1–5, particularly in the CXCR2 receptor, is proposed based on various analyses. Results from ^{1}H NMR validation supported the docking values obtained for R^2. Additionally, Density Functional Theory (DFT) studies were conducted to explore the physical properties of these compounds, confirming the significant activity of compounds 5, 2, and 4. The docking study highlights the potential of these compounds as anticancer agents, with compounds 1, 2, and 5 showing superior efficacy compared to compounds 3, 4. These findings drive ongoing research focused on developing potent anticancer agents through the modification of natural products. Molecular docking and DFT calculations play crucial roles in predicting activity stability and electron properties, aiding in better understanding the compounds' structures. Further investigations are underway to elucidate the mechanisms of action and develop derivatives aimed at enhancing anticancer inhibitory activity.

COMPETING INTERESTS

The authors declare no conflict of interest.

AUTHORS' CONTRIBUTIONS

All authors contribute equally to the manuscript.

ACKNOWLEDGEMENTS

We acknowledge Ho Chi Minh City University of Technology (HCMUT), VNU-HCM for supporting this study.

This research is funded by Vietnam National University HoChiMinh City (VNU-HCM) under grant number: DS2025-20-13

REFERENCES

1. Habtemariam S. Natural Products in Alzheimer's Disease Therapy: Would Old Therapeutic Approaches Fix the Broken Promise of Modern Medicines? Molecules (Basel, Switzerland). 2019;24(8):1519. Available from: https://10.3390/molecules24081519.
2. Hamaguchi T, Ono K, Yamada M. REVIEW: curcumin and Alzheimer's disease. CNS Neuroscience {&} Therapeutics. 2010;16(5):285–97. Available from: https://10.1111/j.1755-5949.2010.00147.x.
3. Hewlings SJ, Kalman DS. Curcumin: A Review of Its Effects on Human Health. Foods. 2017;6(10):92. Available from: https://10.3390/foods6100092.
4. Sandur SK, Pandey MK, Sung B, Ahn KS, Murakami A, Sethi G, et al. Curcumin, demethoxycurcumin, bisdemethoxycurcumin, tetrahydrocurcumin and turmerones differentially regulate anti-inflammatory and anti-proliferative responses through a ROS-independent mechanism. Carcinogenesis. 2007;28(8):1765–73. Available from: https://10.1093/carcin/bgm123.

Table 2: Quantum chemical characteristics of the molecules in a vacuum

Comp.	EaHOMO	EaLUMO	IEa	EAa	Eagap	⊠a	Sb	χa	μc
1	-5,47	-1,81	5,47	1,81	3,66	3,64	0,27	3,64	0,88
2	-5,2	-1,8	5,2	1,8	3,4	3,5	0,29	3,5	2,74
3	-5,76	-1,9	5,76	1,9	3,86	3,83	0,26	3,83	2,08
4	-5,54	-1,9	5,54	1,9	3,64	3,72	0,27	3,72	2,26
5	-5,22	-0,74	5,22	0,74	4,48	2,98	0,33	2,98	3,89

a: in eV, b: in eV-1, c: in Debye.

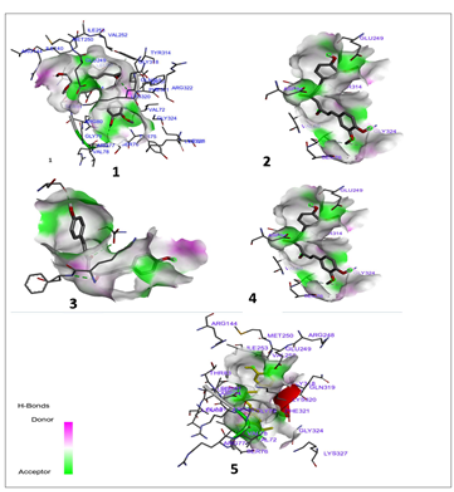

Figure 5: Pocket site with H-Bonds of compounds and the receptor. *[Source: Authors]*

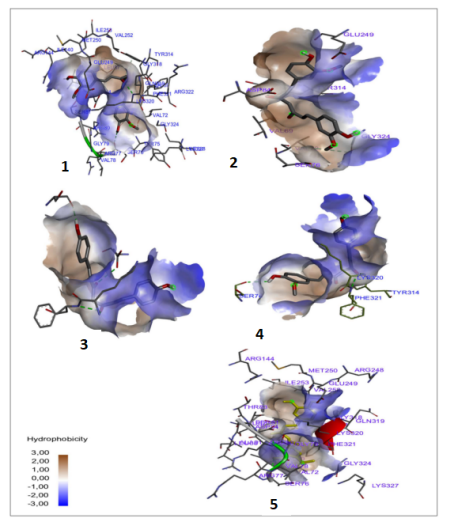

Figure 6: The connect regioncontains hydrophobic and hydrophilic sites. *[Source: Authors]*

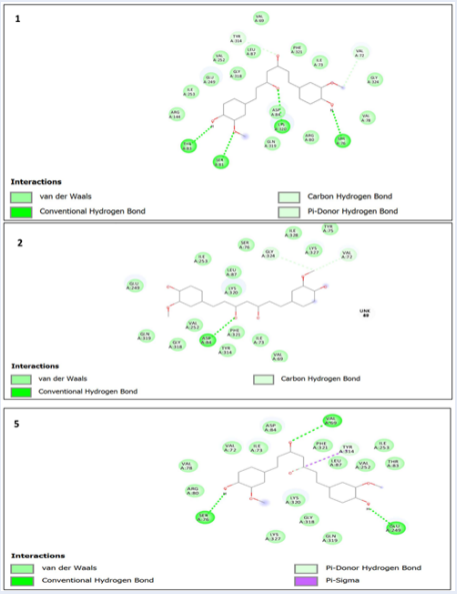

Figure 7: Two dimensions with the interaction of compounds in the study. *[Source: Authors]*

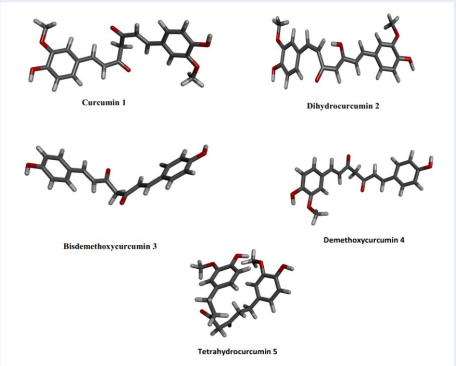

Figure 3: The optimized structure of compounds under study. *[Source: Authors]*

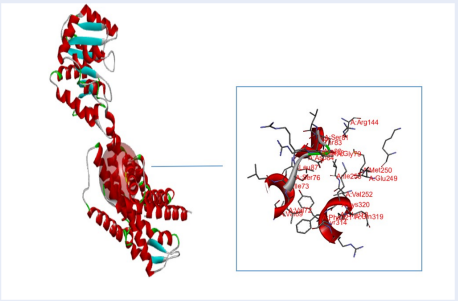

Figure 4: Structure andactive site of CXCR2. *[Source: Authors]*

5. Tomeh MA, Hadianamrei R, Zhao X. A Review of Curcumin and Its Derivatives as Anticancer Agents. International Journal of Molecular Sciences. 2019;20(5):1033. Available from: https://10.3390/ijms20051033.
6. Lai CS, Ho CT, Pan MH. The Cancer Chemopreventive and Therapeutic Potential of Tetrahydrocurcumin. Biomolecules. 2020;10(6):831. Available from: https://10.3390/biom10060831.
7. Aggarwal BB, Deb L, Prasad S. Curcumin differs from tetrahydrocurcumin for molecular targets, signaling pathways and cellular responses. Molecules (Basel, Switzerland). 2014;20(1):185–205. Available from: https://10.3390/molecules20010185.
8. Y G, Molecules, et al. Tetrahydrocurcumin derivatives Enhanced the Anti-Inflammatory activity of curcumin: synthesis, biological evaluation, and Structure–Activity relationship analysis. MDPI. 2023;Available from: https://doi.org/10.3390/molecules28237787.
9. Garcia-Marcos M. Heterotrimeric G protein signaling without GPCRs: the Gα-binding-and-activating (GBA) motif. The Journal of Biological Chemistry. 2024;300(3). Available from: https://10.1016/j.jbc.2024.105756.
10. Lazennec G, Rajarathnam K, Richmond A. CXCR2 chemokine receptor - a master regulator in cancer and physiology. Trends in Molecular Medicine. 2024;30(1):37–55. Available from: https://10.1016/j.molmed.2023.09.003.
11. Veenstra M, Ransohoff RM. Chemokine receptor CXCR2: physiology regulator and neuroinflammation controller? Journal of Neuroimmunology. 2012;246(1-2):1–9. Available from: https://10.1016/j.jneuroim.2012.02.016.
12. Plata RE, Singleton DA. A case study of the mechanism of alcohol-mediated Morita Baylis-Hillman reactions. The importance of experimental observations. Journal of the American Chemical Society. 2015;137(11):3811–26. Available from: https://10.1021/ja5111392.
13. Salman AW, Haque RA, Kadhim MM, Malan FP, Ramasami P. Novel triazine-functionalized tetra-imidazolium hexafluorophosphate salt: Synthesis, crystal structure and DFT study. Journal of Molecular Structure. 2019;1198. Available from: https://10.1016/j.molstruc.2019.126902.
14. Bursch M, Mewes JM, Hansen A, Grimme S. Best-Practice DFT Protocols for Basic Molecular Computational Chemistry. Angewandte Chemie International Edition in English. 2022;61(42). Available from: https://10.1002/anie.202205735.
15. Neese F. The ORCA program system. Wiley Interdisciplinary Reviews Computational Molecular Science. 2011;2(1):73–8. Available from: https://10.1002/wcms.81.
16. Parr RG, Pearson RG. Absolute hardness: companion parameter to absolute electronegativity. Journal of the American Chemical Society. 1983;105(26):7512–6. Available from: https://10.1021/ja00364a005.
17. Sayin K, Kariper SE, Taştan M, Sayin TA, Karakaş D. Investigations of structural, spectral, electronic and biological properties of N-heterocyclic carbene Ag(I) and Pd(II) complexes. Journal of Molecular Structure. 2019;1176:478–87. Available from: https://10.1016/j.molstruc.2018.08.103.
18. Hussein HA, Kassim MN, Maulidiani M, Abas F, Abdullah MA. Cytotoxicity and 1H NMR metabolomics analyses of microalgal extracts for synergistic application with Tamoxifen on breast cancer cells with reduced toxicity against Vero cells. Heliyon. 2022;8(3). Available from: https://10.1016/j.heliyon.2022.e09192.
19. Dennis J, Moré J. Quasi-Newton Methods, Motivation and Theory. SIAM Review. 1977;19(1):46–89. Available from: https://10.1137/1019005.
20. Kim S, Chen J, Cheng T, Gindulyte A, He J, He S, et al. PubChem in 2023: new data content and improved web interfaces. Nucleic Acids Research. 2023;51:1373–80. Available from: https://10.1093/nar/gkac956.

VNUHCM Journal of Engineering and Technology 2026,(2): 2800-2810

Open Access Full Text Article

Bài báo nghiên cứu

Nghiên cứu tiềm năng chống ung thư của curcumin và dẫn chất trên thụ thể CXCR2

Lê Vũ Phúc , Trần Thị Thu Hạnh *

Use your smartphone to scan this QR code and download this article

TÓM TẮT

Các hợp chất tự nhiên có tiềm năng ứng dụng trong điều trị các bệnh lý nan y như ung thư đang ngày càng thu hút được sự chú ý trong nghiên cứu y học. Việc sử dụng các phương pháp mô phỏng tính toán ngày càng trở nên phổ biến hơn trong việc nghiên cứu các hợp chất này, tạo điều kiện thuận lợi cho việc lựa chọn các khung phân tử có triển vọng cho mục đích điều trị. Curcumin, một phân tử có nhiều cấu trúc tương tự và được biến đổi, được sử dụng để dự đoán các hợp chất dược phẩm tiềm năng bằng các phương pháp tính toán phân tử. Nghiên cứu này nhằm mục đích sử dụng một số cấu trúc, bao gồm curcumin, demethoxycurcumin (DMC), bisdemethoxycurcumin (BDMC), dihydrocurcumin (DHC) và đặc biệt là tetrahydrocurcumin (THC), để dự báo khả năng ức chế thụ thể CXCR2 thông qua DFT và phương pháp docking. Trong bài viết này, phương pháp Lý thuyết hàm mật độ (DFT) sẽ được sử dụng để tối ưu hóa cấu trúc và tính toán các tham số lượng tử khác nhau. Sau đó, dựa vào cấu trúc được tối ưu sẽ được dự đoán quang phổ 1H NMR và so sánh với dữ liệu thực nghiệm để đánh giá mức độ gần với thực tế. Các phối tử sẽ được gắn với protein CXCR2 để đánh giá tác động của chúng lên protein này. Kết quả cho ta thấy được hiệu quả ức chế đáng chú ý của THC trên CXCR2, được hỗ trợ bởi sự hình thành liên kết pi-sigma trong túi liên kết của thụ thể. Những phát hiện này sẽ tạo tiền đề cho các nghiên cứu sắp tới trên THC trở thành một ứng cử viên dược phẩm tiềm năng trong tương lai. Bài viết này bao gồm các phần sau: phần giới thiệu cung cấp cái nhìn tổng quan về các phân tử tự nhiên được gọi là phối tử và protein mục tiêu; phần phương pháp tính toán phác thảo các kỹ thuật tính toán sẽ được sử dụng trong nghiên cứu bao gồm DFT và lắp ghép phân tử với phần mềm Autodock Vina; và phần kết quả trình bày những phát hiện thu được trong quá trình nghiên cứu.

Từ khoá: Thiết kế thuốc, docking phân tử, hợp chất tự nhiên, dẫn xuất curcumin, ức chế CXCR2

Khoa Khoa học Ứng dụng, Trường Đại học Bách Khoa – Đại học Quốc gia TP. Hồ Chí Minh (HCMUT), TP. Hồ Chí Minh, Việt Nam

Liên hệ

Trần Thị Thu Hạnh , Khoa Khoa học Ứng dụng, Trường Đại học Bách Khoa – Đại học Quốc gia TP. Hồ Chí Minh (HCMUT), TP. Hồ Chí Minh, Việt Nam

Email: thuhanhsp@hcmut.edu.vn

Lịch sử

- Ngày nhận: 23-8-2024
- Ngày sửa đổi: 28-7-2025
- Ngày chấp nhận: 21-10-2025
- Ngày đăng: 07-05-2026

DOI : https://doi.org/10.32508/vnuhcmj-et.v9i1.1437

VNUHCM PRESS

Trích dẫn bài báo này: L V P, T T T H. **Nghiên cứu tiềm năng chống ung thư của curcumin và dẫn chất trên thụ thể CXCR2**. *VNUHCM J. Eng. Technol.* 2026; (2):2800-2810.